World Journal of Gastroenterology

Submit a Manuscript: https://www.f6publishing.com

*World J Gastroenterol* 2021 December 28; 27(48): 8323-8342

DOI: 10.3748/wjg.v27.i48.8323

ISSN 1007-9327 (print) ISSN 2219-2840 (online)

ORIGINAL ARTICLE

Basic Study

# Dual therapy with zinc acetate and rifaximin prevents from ethanol-induced liver fibrosis by maintaining intestinal barrier integrity

Yuki Fujimoto, Kosuke Kaji, Norihisa Nishimura, Masahide Enomoto, Koji Murata, Soichi Takeda, Hiroaki Takaya, Hideto Kawaratani, Kei Moriya, Tadashi Namisaki, Takemi Akahane, Hitoshi Yoshiji

**ORCID number:** Yuki Fujimoto 0000-0002-5046-0588; Kosuke Kaji 0000-0002-1822-6759; Norihisa Nishimura 0000-0002-6295-3283; Masahide Enomoto 0000-0001-8980-4758; Koji Murata 0000-0001-5149-2437; Soichi Takeda 0000-0001-6457-2954; Hiroaki Takaya 0000-0002-4990-7573; Hideto Kawaratani 0000-0002-4361-0592; Kei Moriya 0000-0002-2878-8296; Tadashi Namisaki 0000-0002-3158-5318; Takemi Akahane 0000-0002-6675-0475; Hitoshi Yoshiji 0000-0002-5243-8544.

**Author contributions:** Fujimoto Y and Kaji K designed the research study; Fujimoto Y, Kaji K, Nishimura N, Enomoto M, Murata K, Takeda S, Takaya H and Kawaratani H performed the research; Moriya K, Namisaki T and Akahane T offered new reagents, analytic tools and material support; Fujimoto Y and Kaji K analyzed the data and wrote the manuscript; Yoshiji H supervised this study; All authors have read and approve the final manuscript.

**Institutional review board statement:** The study was reviewed and approved by the Institutional review board of Nara Medical University, Kashihara, Japan (authorization numbers: 12734).

**Yuki Fujimoto, Kosuke Kaji, Norihisa Nishimura, Masahide Enomoto, Koji Murata, Soichi Takeda, Hiroaki Takaya, Hideto Kawaratani, Kei Moriya, Tadashi Namisaki, Takemi Akahane, Hitoshi Yoshiji,** Department of Gastroenterology, Nara Medical University, Kashihara 6348521, Nara, Japan

**Corresponding author:** Kosuke Kaji, MD, PhD, Doctor, Lecturer, Senior Researcher, Department of Gastroenterology, Nara Medical University, 840, Shijo-cho, Kashihara 6348521, Nara, Japan. kajik@naramed-u.ac.jp

## Abstract

### *BACKGROUND*

Hepatic overload of gut-derived lipopolysaccharide dictates the progression of alcoholic liver disease (ALD) by inducing oxidative stress and activating Kupffer cells and hepatic stellate cells through toll-like receptor 4 signaling. Therefore, targeting the maintenance of intestinal barrier integrity has attracted attention for the treatment of ALD. Zinc acetate and rifaximin, which is a nonabsorbable antibiotic, had been clinically used for patients with cirrhosis, particularly those with hepatic encephalopathy, and had been known to improve intestinal barrier dysfunction. However, only few studies focused on their efficacies in preventing the ALD-related fibrosis development.

### *AIM*

To investigate the effects of a combined zinc acetate with rifaximin on liver fibrosis in a mouse ALD model.

### *METHODS*

To induce ALD-related liver fibrosis, female C57BL/6J mice were fed a 2.5% (v/v) ethanol-containing Lieber-DeCarli liquid diet and received intraperitoneal carbon tetrachloride ($CCl_4$) injection twice weekly (1 mL/kg) for 8 wk. Zinc acetate (100 mg/L) and/or rifaximin (100 mg/L) were orally administered during experimental period. Hepatic steatosis, inflammation and fibrosis as well as intestinal barrier function were evaluated by histological and molecular analyses. Moreover, the direct effects of both agents on Caco-2 barrier function were assessed by *in vitro* assays.

### *RESULTS*

**Conflict-of-interest statement:** All authors have nothing to disclose.

**Data sharing statement:** No additional data are available.

**Country/Territory of origin:** Japan

**Specialty type:** Gastroenterology and hepatology

**Provenance and peer review:** Unsolicited article; Externally peer reviewed

**Peer-review model:** Single blind

**Peer-review report's scientific quality classification**
Grade A (Excellent): A
Grade B (Very good): 0
Grade C (Good): C
Grade D (Fair): 0
Grade E (Poor): 0



**Received:** July 6, 2021
**Peer-review started:** July 6, 2021
**First decision:** July 26, 2021
**Revised:** July 6, 2021
**Accepted:** December 10, 2021
**Article in press:Published online:** December 28, 2021

**P-Reviewer:** Wang QY
**S-Editor:** Liu M
**L-Editor:** A
**P-Editor:** Liu M

In the ethanol plus $CCl_4$-treated mice, combination of zinc acetate and rifaximin attenuated oxidative lipid peroxidation with downregulation of *Nox2* and *Nox4*. This combination significantly inhibited the Kupffer cells expansion and the proinflammatory response with blunted hepatic exposure of lipopolysaccharide and the toll-like receptor 4/nuclear factor kB pathway. Consequently, liver fibrosis and hepatic stellate cells activation were efficiently suppressed with downregulation of *Mmp-2, -9, -13, and Timp1*. Both agents improved the atrophic changes and permeability in the ileum, with restoration of tight junction proteins (TJPs) by decreasing the expressions of tumor necrosis factor α and myosin light chain kinase. In the *in vitro* assay, both agents directly reinforced ethanol or lipopolysaccharide-stimulated paracellular permeability and upregulated TJPs in Caco-2 cells.

*CONCLUSION*
Dual therapy with zinc acetate and rifaximin may serve as a strategy to prevent ALD-related fibrosis by maintaining intestinal barrier integrity.

**Key Words:** Liver fibrosis; Intestinal permeability; Alcoholic liver disease; Lipopolysaccharide; Toll-like receptor; Tight junction protein



**Core Tip:** Gut-derived lipopolysaccharide dictates the progression of alcoholic liver disease (ALD) hence the maintenance of intestinal barrier integrity has attracted attention for the treatment of ALD. This study elucidates the preventive effect of combined zinc supplementation and rifaximin from ALD-related liver fibrosis induced by ethanol plus carbon tetrachloride in mice. This effect is involved in the multifaceted regulatory functions that maintain intestinal barrier integrity and reduce hepatic lipopolysaccharide exposure, thereby, leading to Kupffer cell expansion and hepatic stellate cell activation by inhibiting the toll-like receptor 4 pathway, highlighting that this regimen may represent a potential novel strategy against ALD-related liver fibrosis.

**Citation:** Fujimoto Y, Kaji K, Nishimura N, Enomoto M, Murata K, Takeda S, Takaya H, Kawaratani H, Moriya K, Namisaki T, Akahane T, Yoshiji H. Dual therapy with zinc acetate and rifaximin prevents from ethanol-induced liver fibrosis by maintaining intestinal barrier integrity. *World J Gastroenterol* 2021; 27(48): 8323-8342
**URL:** https://www.wjgnet.com/1007-9327/full/v27/i48/8323.htm
**DOI:** https://dx.doi.org/10.3748/wjg.v27.i48.8323

## INTRODUCTION

Alcoholic liver disease (ALD), which is the most common and serious complication of excessive alcohol consumption, includes a spectrum of disorders, such as acute or chronic hepatitis, fatty liver disease, cirrhosis, and hepatocellular carcinoma[1,2]. The increasing mortality from ALD has become a major health problem in both Western and Asian countries[3]. Currently, limiting alcohol intake remains the most effective therapy for patients in all stages of ALD, although only few individuals succeed in substantially abstaining from alcohol consumption. Therefore, novel efficacious medications are urgently required to prevent the development of ALD.

ALD is known to progress through several communications between the liver and several physiologic systems in other organs[4,5]. Among various factors that mediate these cross-talks, the gut-derived endotoxin lipopolysaccharide (LPS), which is produced by gram-negative bacteria, particularly plays a pivotal role in inflammation and fibrosis in ALD[6]. Accumulation of LPS in response to alcohol consumption may be attributed to the functional impairment of intestinal barrier integrity, including intestinal hyperpermeability secondary to disrupted tight junction[7]. LPS is transported into the liver and activates Kupffer cells and macrophages that had been recruited in the liver through toll-like receptor 4 (TLR4) and its coreceptor CD14,

which in turn force these cells to produce inflammatory cytokines[8]. Moreover, gut-derived LPS triggers hepatic stellate cell (HSC) activation by increasing its susceptibility to acetaldehyde and transforming growth factor (TGF)-b and leading to extracellular matrix (ECM) deposition, intrahepatic inflammation, and fibrosis[9]. Therefore, maintenance of intestinal barrier integrity and blockage of the transfer of LPS from the intestine to the liver may be a therapeutic strategy to prevent alcohol-induced liver fibrosis.

Zinc is the second most abundant trace metal in humans after iron and is the only metal that appears in all enzyme classes[10]. Zinc deficiency is often observed in patients with ALD and usually becomes evident with increasing severity and with the progression of ALD from steatosis to cirrhosis[11,12]. Zinc supplementation in patients with cirrhosis provides metabolic effects that assist in the improvement of liver function, hepatic encephalopathy, and nutritional status[13-15]. Notably, Zhong *et al*[16] have documented that zinc deficiency induced by chronic alcohol exposure augmented epithelial barrier dysfunction with subsequent increase in gut permeability and development of endotoxemia in alcoholic liver injury. Meanwhile, several animal studies have shown that zinc supplementation could ameliorate intestinal barrier dysfunction[17,18]. However, supplementation with zinc alone was considered to only partially improve the outcome of patients with chronic liver diseases, including ALD [19]. Therefore, we postulated that a combination of zinc and another agent with antifibrotic effects would add benefits in the treatment of alcohol-induced liver fibrosis.

Rifaximin is an antibiotic that is minimally absorbed, has broad-spectrum activity against gram-positive and gram-negative aerobic and anaerobic enteric bacteria, and is clinically available for hepatic encephalopathy or travelers' diarrhea[20,21]. Our recent clinical studies have elucidated that rifaximin significantly decreased serum endotoxin activity and potentially improved intestinal permeability without modifying the gut microbiome in patients with cirrhosis[22]. Moreover, a recent study demonstrated that rifaximin inhibited toxin-induced apoptosis and deprivation of tight junction proteins (TJPs) in human intestinal cells through pregnane X receptor (PXR)-dependent inhibition of the TLR4/MyD88/nuclear factor kB (NF-kB) pathway[23]. However, the therapeutic potential of rifaximin against alcohol-induced liver fibrosis had been obscure.

This study aimed to investigate the combined effects of zinc supplementation and rifaximin on liver fibrosis induced by ethanol plus carbon tetrachloride ($CCl_4$) in connection with their protective properties against intestinal barrier disruption.

## MATERIALS AND METHODS

### *Animals and experimental protocol*

Ten-week-old female C57BL/6J mice (CLEA Japan, Osaka, Japan) were housed under 23 °C ± 3 °C with 50% ± 20% humidity and a 12-h light/12-h dark cycle. All experiments were performed over an 8-wk period, since our previous report has shown that administration of ethanol plus $CCl_4$ for this period definitely developed ALD-related liver fibrosis[24].

The mice were divided into five treatment groups (Figure 1). The control group (C/V; $n$ = 10) were fed non-ethanol liquid diet (Research Diets, New Brunswick, NJ, United States). The E/V group ($n$ = 10) were fed a 2.5% (v/v) ethanol-containing Lieber–DeCarli liquid diet (research diets) and received intraperitoneal injection of $CCl_4$ (FUJIFILM, Wako Pure Chemical Corporation, Osaka, Japan) twice a week (1 mL/kg body weight)[25]. The E/Zn ($n$ = 10) and E/RFX ($n$ = 10) groups were fed ethanol diet with 100 mg/L of zinc acetate (FUJIFILM, Wako Pure Chemical Corporation) and 100 mg/L of rifaximin (ASKA Pharmaceutical Co. Ltd., Tokyo, Japan), respectively[26,27], and received intraperitoneal $CCl_4$ injection twice weekly. The E/both group ($n$ = 10) were fed ethanol diet that contained a combination of zinc acetate and rifaximin and received intraperitoneal $CCl_4$ injection. The same amount of lactose hydrate (FUJIFILM, Wako Pure Chemical Corporation) was used as vehicle for the C/V and E/V groups. Another set of mice groups were used to measure intestinal permeability, as described in Measurement of *in vivo* intestinal permeability. For sample collection, all mice underwent the following procedures: anesthesia with barbiturate overdose (intravenous injection, 150 mg/kg pentobarbital sodium), blood collection from the cervical artery and harvesting of the liver and ileum immediately after sacrifice. Serum biologic markers were measured by SRL, Inc. (Tokyo, Japan). The animal care and experimental procedures were approved by the ethics committee of

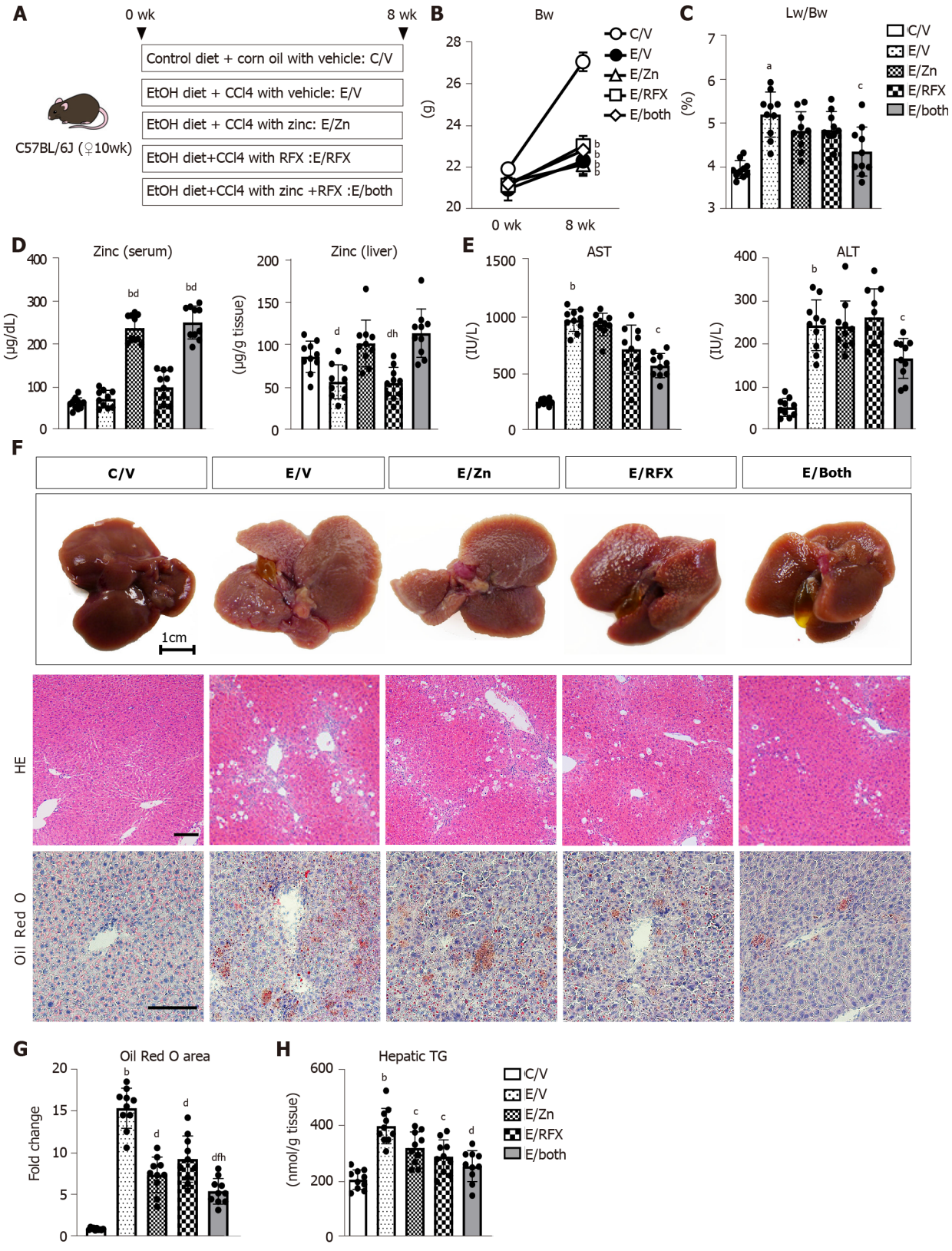


**Figure 1 Zinc acetate and rifaximin against hepatic steatosis in alcoholic liver disease mice.** A: Experimental protocols; B: Changes in body weights during experimental period; C: Ratio of liver weight to body weight at the end of experiment; D: Zinc concentrations of the serum (left) and the liver (right); E: Serum levels of aspartate aminotransferase (left) and alanine aminotransferase (right); F: Representative macroscopic appearances (upper), microphotographs of hematoxylin and eosin (middle) and Oil Red O staining (lower) of the livers in the experimental mice. Scale bar: 25 μm; G: Semi-quantification of lipid accumulation stained by Oil Red O in high-power field by NIH imageJ software. Histochemical quantitative analyses included five fields per section. Quantitative values are indicated as fold changes to the values of C/V group; H: Hepatic concentrations of triglyceride. Data are mean ± SD ($n$ = 10), $^{a}P < 0.05$ and $^{b}P < 0.01$ *vs* C/V group; $^{c}P < 0.05$ and $^{d}P < 0.01$ *vs* E/V group; $^{e}P < 0.05$ and $^{f}P < 0.01$ *vs* E/Zn group; $^{g}P < 0.05$ and $^{h}P < 0.01$ *vs* E/RFX group. AST: Aspartate aminotransferase; ALT: Alanine aminotransferase; HE: Hematoxylin and eosin.

Experimental Animal Care of Nara Medical University, Kashihara, Japan (authorization numbers: 12734).

### Histologic and immunohistochemical analyses

The liver and ileum specimens were fixed in 10% formalin and embedded in paraffin, and other liver specimens were fixed with 4% paraformaldehyde for 24 h, then frozen in a Cryomold with Tissue-Tek OCT compound (Sakura Finetek Japan, Tokyo, Japan) for frozen sections. Paraffin-embedded sections of 5-μm thickness were stained with hematoxylin and eosin (HE) for the liver and ileum and with Sirius Red for the liver and frozen liver sections were stained with Oil Red O at Narabyouri Research Co. (Nara, Japan). To evaluate the morphologic changes in the ileum, 10 well-oriented crypt–villus units were examined per slide under a microscope. Immunohistochemistry was performed as described previously and α-smooth muscle actin (SMA) (#ab5694; 1:200, Abcam, Cambridge, United Kingdom), F4/80 (#ab100790; 1:100, Abcam) and COL-1 (#14695-1-AP; 1:500, Proteintech, Rosemont, IL, United States) were used as primary antibodies[28,29]. Immunofluorescence test for zonula occludens-1 (ZO-1) (#61-7300; 1:250, Invitrogen, Carlsbad, CA, United States) and Occludin (#ab216327; 1:200, Abcam) was performed on the paraffin-embedded ileum sections. Primary antibodies were detected using Alexa Fluor-conjugated secondary antibodies (Invitrogen). Images were captured using a BX53 (Olympus, Tokyo, Japan) for histology and immunohistochemistry and a BZ-X700 (Keyence, Osaka, Japan) for immunofluorescence. Semiquantitative analysis was performed using Image J software version 64 (National Institutes of Health, Bethesda, MD, United States).

### Intrahepatic zinc and triglyceride concentration

Intrahepatic zinc and triglyceride concentrations were measured in 100 mg of frozen liver tissue per mouse using the Metalloassay Kit (Metallogenics, Chiba, Japan) and Triglyceride-Glo™ Assay (Promega, Madison, WI, United States), respectively, according to the manufacturer's instructions.

### Intrahepatic alcohol dehydrogenase 1, aldehyde dehydrogenase 2 and cytochrome P450 2E1 (CYP2E1) activity

Intrahepatic alcohol dehydrogenase 1 (ADH1) and aldehyde dehydrogenase 2 (ALDH2) activities were measured by using Alcohol Dehydrogenase Activity Colorimetric Assay Kit (BioVision, Milpitas, CA, United States) and ALDH2 activity assay kit (Abcam), respectively, according to the manufacturer's instructions. Intrahepatic CYP2E1 activity was determined by measuring the hydroxylation of *p*-nitrophenol in whole liver extract as described[30].

### Intrahepatic catalase, superoxide dismutase, and malondialdehyde concentration

Intrahepatic levels of catalase (CAT), superoxide dismutase (SOD) and malondialdehyde (MDA) were measured in 25 mg frozen liver tissue in each mouse using Mouse catalase ELISA Kit (CUnited StatesBIO, Houston, TX, United States), Mouse Super Oxidase Dimutase, SOD ELISA Kit (CUnited StatesBIO) and OxiSelect™ TBARS Assay Kit (Cell Biolabs, Inc., San Diego, CA, United States), according to the manufacturer's protocol.

### Mouse matrix metalloproteinase-9 activity assay

Intrahepatic matrix metalloproteinase (MMP)-9 activities were evaluated in frozen liver tissue per mouse by the Mouse MMP-9 Activity Assay Kit (QuickZyme Biosciences, Leiden, Netherlands), according to the manufacturers protocol.

### Measurement of in vivo intestinal permeability

*In vivo* intestinal permeability was determined as previously described with brief modifications[31]. Six hours after initiating fasting conditions, the mice ($n$ = 5) were orally given 600 mg/kg body weight of fluorescein isothiocyanate (FITC)-dextran (4 kDa) (TdB Labs, Uppsala, Sweden). Blood was collected from the portal vein 4 h after FITC-dextran administration. To evaluate the degree of gut permeability, plasma was analyzed by fluorescence measurement of the concentration of FITC-labeled dextran at an excitation wavelength of 490 nm and an emission wavelength of 520 nm.

### Cell culture

To explore *in vitro* effects of zinc acetate and rifaximin on enterocytes, we used the human colorectal adenocarcinoma line Caco-2. Caco-2 cells were obtained from Riken

BRC Cell Bank (Ibaraki, Japan) and were cultured, as described previously[32]. The cells were cultured in Dulbecco's modified Eagle's medium supplemented with 100 U/mL of penicillin, 100 g/mL of streptomycin, 0.1-mM nonessential amino acids, 10-mM HEPES, and 10% fetal bovine serum at 37 °C in an environment with 5% carbon dioxide. Culture medium was replaced every 2 d. Caco-2 cells were subcultured after partial digestion with 0.25% trypsin-EDTA, and passages 19–30 were used. For alcohol intoxication, 5% ethanol was added to the culture medium for 3 h, with or without the addition of different concentrations of zinc acetate (1−100 μM) and/or rifaximin (0.1−10 μM) 30 min before alcohol intoxication. A previous report has shown that 5% ethanol significantly affected the Caco-2 monolayer barrier function[33]. For tumor necrosis factor (TNF)α stimulation, recombinant human TNFα (100 ng/mL, Abcam) was added to the Caco-2 cell monolayers for 6 h, with or without zinc acetate (100 μM) or rifaximin (10 μM) 30 minutes prior. For LPS stimulation, LPS (O55:B5) (2 μg/mL; Sigma-Aldrich, St. Louis, MO, United States) was added to the Caco-2 cell monolayers with and without zinc acetate (100 μM) or rifaximin (10 μM) for 24 h. The phosphoinositide 3-kinase (PI3K) inhibitor LY294002 (10 μM, ChemScene, Monmouth Junction, NJ, United States) or the human PXR antagonist, SPA70 (510 μM, Axon Medchem, Groningen, Netherlands) was added to the culture media that had been treated with zinc acetate or rifaximin, respectively[34,35].

### Measurement of transepithelial electrical resistance

To assess the *in vitro* Caco-2 monolayer barrier function, we measured the transepithelial electrical resistance (TEER) using an electrical resistance system (Millicell-ERS®; Millipore Corporation, Bedford, MA, United States), as reported previously[36]. The electrical resistance was expressed in units of Ω/cm$^2$ using the surface area of the Trans-well insert.

### Cell viability assay

*In vitro* cell viability was determined using the Premix WST-1 Cell Proliferation Assay system (Takara Bio, Kusatsu, Japan), according to the manufacturer's protocol. Cell viability was calculated as the relative value to the start of exposure to each agent.

### Quantitative real-time polymerase chain reaction assay

Total RNA was extracted from the liver and ileum tissues and cultured Caco-2 cells using the RNeasy Mini Kit (Qiagen, Hilden, Germany). After assessing the quality and concentration, 2 μg of total RNA was subjected to cDNA synthesis using the High-Capacity RNA-to-cDNA kit (Applied Biosystems, Foster City, CA, United States). Quantitative real-time polymerase chain reaction (qRT-PCR) with gene-specific primer pairs (Supplementary Table 1) was performed using the StepOnePlus Real-time PCR system and SYBR Green (Applied Biosystems). The levels of mRNA expression were normalized according to the internal control of the housekeeping gene glyceraldehyde 3-phosphate dehydrogenase. All reactions were performed using 1:10 diluted cDNA; mRNA expression levels were estimated using the $2^{-\Delta\Delta CT}$ method and were presented as fold changes relative to the controls for each experiment.

### Protein extraction and western blotting

Proteins were extracted from frozen liver tissues and Caco-2 cells using T-PER Tissue Protein Extraction Reagent supplemented with proteinase and phosphatase inhibitors (Thermo Scientific, Rockford, IL, United States). Western blot was performed, as described previously[37]. The membranes were incubated overnight with antibodies against phospho-IKKα/β (Ser176/180) (#2697; Cell Signaling Technology, Danvers, MA, United States), IKKβ (#2370; CST), IkBα (#4812; CST), NF-kB p65 (#8242; CST), phospho-NF-kB p65 (Ser536) (#3033; CST), COL-1 (#14695-1-AP; Proteintech), ZO-1 (#61-7300; Invitrogen), Occludin (#ab216327; Abcam), AKT (#9272; CST), phospho-AKT (Ser473) (#9271; CST), and β actin (#4967). Densitometric analysis was performed using ImageJ software version 64.

### Statistical analyses

Continuous variables are presented as mean ± SD. Statistical significance was analyzed with a 2-sided Student's *t*-test or one-way analysis of variance, followed by Bonferroni's multiple comparison test, as appropriate. Statistical analyses were performed using Prism, version 9.1.2 (GraphPad Software, La Jolla, CA, United States). *P* values of < 0.05 were considered to indicate statistical significance.

## RESULTS

### *Combination of zinc acetate and rifaximin improved liver dysfunction and suppressed hepatic steatosis in ethanol plus $CCl_4$-treated mice.*

Figure 1A shows our initial examination of the effects of zinc acetate and rifaximin on ALD-related fibrosis induced *via* combined ethanol and $CCl_4$ administration in mice. After 8 wk, the administration of ethanol plus $CCl_4$ group had remarkable delay in body weight gain, compared with that in the control group, and this delay in body weight gain could not be prevented by treatments with zinc acetate and rifaximin (Figure 1B). Conversely, the relative liver weights increased in the ethanol plus $CCl_4$-treated mice, and combined treatment with zinc acetate and rifaximin efficiently attenuated hepatomegaly (Figure 1C). To confirm the effect of zinc supplementation, we measured the serum and hepatic levels of zinc in the experimental groups. As shown in Figure 1D, the ethanol plus $CCl_4$-treated mice, compared with the control group, showed almost equivalent levels of serum zinc but lower levels of hepatic zinc, and treatment with zinc acetate significantly increased both the serum and hepatic zinc levels in the ethanol plus $CCl_4$-treated mice. Administration of zinc acetate (100 mg/L) and rifaximin (100 mg/L) at the present doses did not cause hypocupremia and renal dysfunction, respectively (Supplementary Figure 1A and B). The serum levels of aspartate aminotransferase (AST) and alanine aminotransferase (ALT) were increased by chronic ethanol exposure and $CCl_4$ administration (Figure 1E). Interestingly, combined treatment with zinc acetate and rifaximin lowered the AST and ALT levels in the ethanol plus $CCl_4$-treated mice (Figure 1E). Serum γ-glutamyl transpeptidase levels were elevated in the ethanol plus $CCl_4$-treated mice and remained unchanged by treatments with both agents (Supplementary Figure 1C). Meanwhile, serum alkaline phosphatase and albumin levels were not affected by chronic ethanol exposure and $CCl_4$ administration (Supplementary Figure 1C). In serum lipid test, serum triglyceride levels were elevated in the ethanol plus $CCl_4$-treated mice that were attenuated by treatments with zinc acetate and rifaximin. However, there were no significant differences in serum total-, high density lipoprotein (HDL)-, and low density lipoprotein (LDL)-cholesterol levels among the experimental groups (Supplementary Figure 1D and E).

Histologic assessment on HE and Oil Red O staining revealed hepatic steatosis in the ethanol plus $CCl_4$-treated mice (Figure 1F and G). Notably, treatment with zinc acetate and rifaximin remarkably attenuated hepatic fat accumulation, and consistently combined treatment with both agents attenuated the hepatic level of triglyceride (Figure 1F-H).

### *Zinc acetate and rifaximin prevented the accumulation of oxidative stress in ethanol plus $CCl_4$-treated mice.*

Next, we evaluated the changes in the activities of metabolic enzymes related to alcohol, acetaldehyde, and cytochrome CYP2E1 in the liver tissues of experimental group. As shown in Figure 2A and B, ethanol and $CCl_4$ administration significantly decreased both ADH1 and ALDH2 activities. Treatment with zinc acetate significantly suppressed the decline of ADH1 activity but did not affect ALDH2 in the ethanol plus $CCl_4$-treated mice. However, neither ADH1 nor ALDH2 activities changed after treatment with rifaximin. CYP2E1 activity was increased in the ethanol plus $CCl_4$-treated mice, and zinc acetate significantly suppressed the increase of CYP2E1 activity but rifaximin did not affected (Figure 2C). These findings indicate that zinc acetate would attenuate CYP2E1-mediated accumulation of oxidative stress.

In the ethanol plus $CCl_4$-treated mice, hepatic levels of antioxidant enzymes CAT and SOD were decreased as compared to control mice, and treatments with zinc acetate and rifaximin significantly prevented the decreases in CAT and SOD levels (Figure 2D and E). The chronic ethanol exposure and $CCl_4$ administration also induced the increase in hepatic levels of MDA, one of the final products of polyunsaturated fatty acids peroxidation (Figure 2F). It was noteworthy that treatments with zinc acetate and rifaximin suppressed the alteration in the levels of MDA (Figure 2F).

Moreover, compared with the control mice, the ethanol plus $CCl_4$-treated mice exhibited higher mRNA levels of the hepatic nicotinamide adenine dinucleotide phosphate oxidase (*Nox*) gene family members (*i.e.*, *Nox1*, *Nox2*, and *Nox4*); treatment with zinc acetate and rifaximin reduced the observed increase in the mRNA levels of *Nox2* and *Nox4* (Figure 2G).

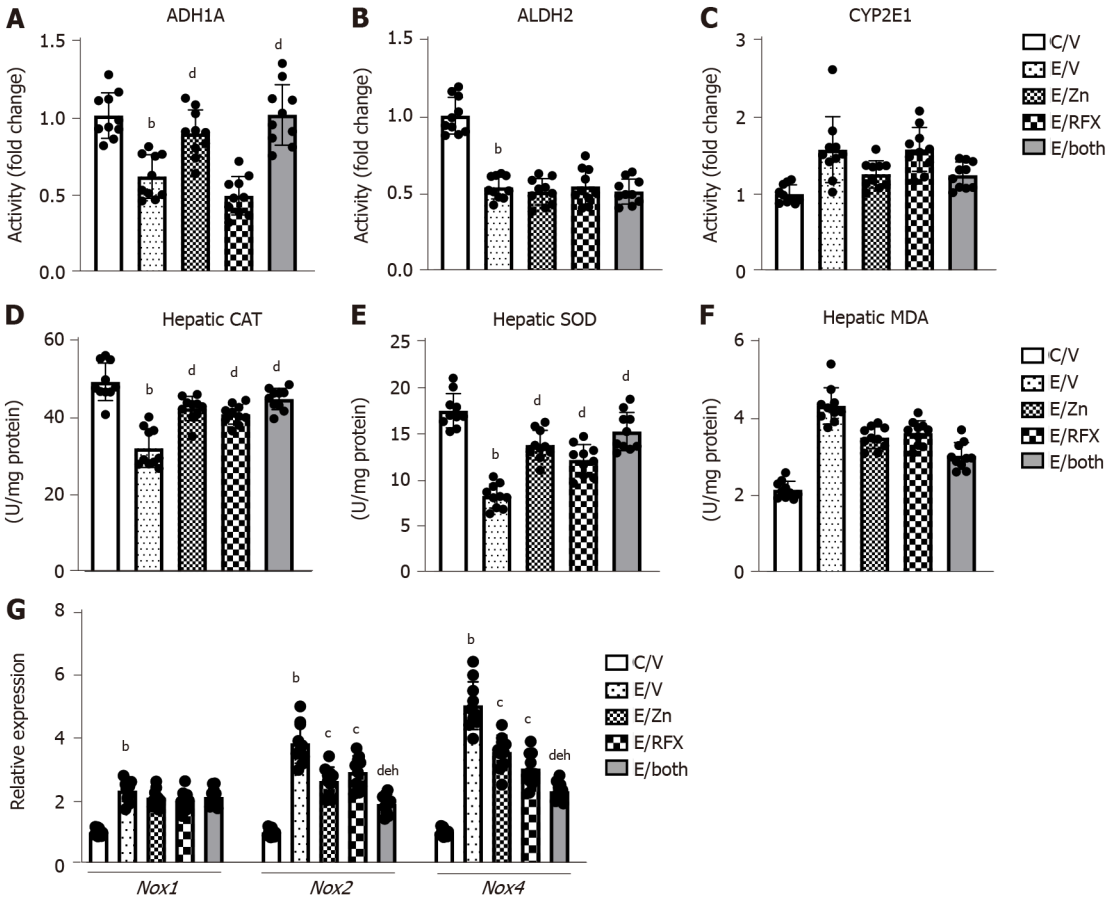


**Figure 2 Zinc acetate and rifaximin on ethanol metabolism and accumulation of oxidative stress in alcoholic liver disease mice.** A-C: Hepatic activity of alcohol dehydrogenase 1 (A), aldehyde dehydrogenase 2 (B) and cytochrome P450 2E1 (CYP2E1) (C). Quantitative values are indicated as fold changes to the values of C/V group; D-F: Hepatic levels of of catalase (D), superoxide dismutase (E) and malondialdehyde (F); G: Relative mRNA expression levels of *Nox1*, *Nox2* and *Nox4* in the liver of experimental mice. The mRNA expression levels were measured by RT-qPCR, and *Gapdh* was used as internal control. Quantitative values are indicated as fold changes to the values of C/V group. Data are mean ± SD ($n$ = 10), $^{a}P$ < 0.05 and $^{b}P$ < 0.01 *vs* C/V group; $^{c}P$ < 0.05 and $^{d}P$ < 0.01 *vs* E/V group; $^{e}P$ < 0.05 and $^{f}P$ < 0.01 *vs* E/Zn group; $^{g}P$ < 0.05 and $^{h}P$ < 0.01 *vs* E/RFX group. ADH1: Alcohol dehydrogenase 1; ALDH2: Aldehyde dehydrogenase 2; CAT: Catalase; SOD: Superoxide dismutase; MDA: Malondialdehyde.

### *Zinc acetate and rifaximin attenuated Kupffer cell expansion and the lipopolysaccharide/TLR4 signaling activation in ethanol plus $CCl_4$-treated mice.*

On the basis of the suppressions in ethanol plus $CCl_4$-induced steatosis and inflammation following zinc acetate and rifaximin treatment, we next evaluated the proinflammatory status of the liver in the experimental mice. We observed extensive infiltration of F4/80-positive Kupffer cells and an increased mRNA levels of *Cd68* in the liver of ethanol plus $CCl_4$-treated mice (Figure 3A–C). Treatment with zinc acetate and rifaximin attenuated the expanded Kupffer cell infiltration and reduced the mRNA expression of *Cd68* which were robustly boosted by combination of the two agents (Figure 3A-C). We also observed that the combination treatment significantly suppressed the increases of M1-polarized macrophages while it had little effect on M2-polarized macrophages in the liver of ethanol plus $CCl_4$-treated mice (Figure 3D and E).

We further assessed to the effect of zinc acetate and rifaximin on the hepatic LPS/TLR4 signaling. Administration of ethanol plus $CCl_4$ caused an upregulation of hepatic LPS-binding protein (LBP), which forms a complex with LPS to interact with the macrophage receptor and initiate a proinflammatory host response (Figure 3F). In accordance with the upregulated hepatic *Lbp* expression, the mRNA levels of *Tlr4* and its coreceptor *Cd14*, which function to detect LPS, were increased in the ethanol plus $CCl_4$-treated mice (Figure 3G). Notably, treatment with zinc acetate and rifaximin ameliorated these increases, suggesting that both agents could reduce the load of LPS to the liver (Figure 3F and G). In the ethanol plus $CCl_4$-treaed mice, the hepatic overload of LPS induced the IKKα/β phosphorylation and in turn promoted the IkBα degradation; NF-kB p65 Levels were consequently increased as a sequence of the LBP/CD14/TLR4 pathway (Figure 3H). The combination of both agents efficiently

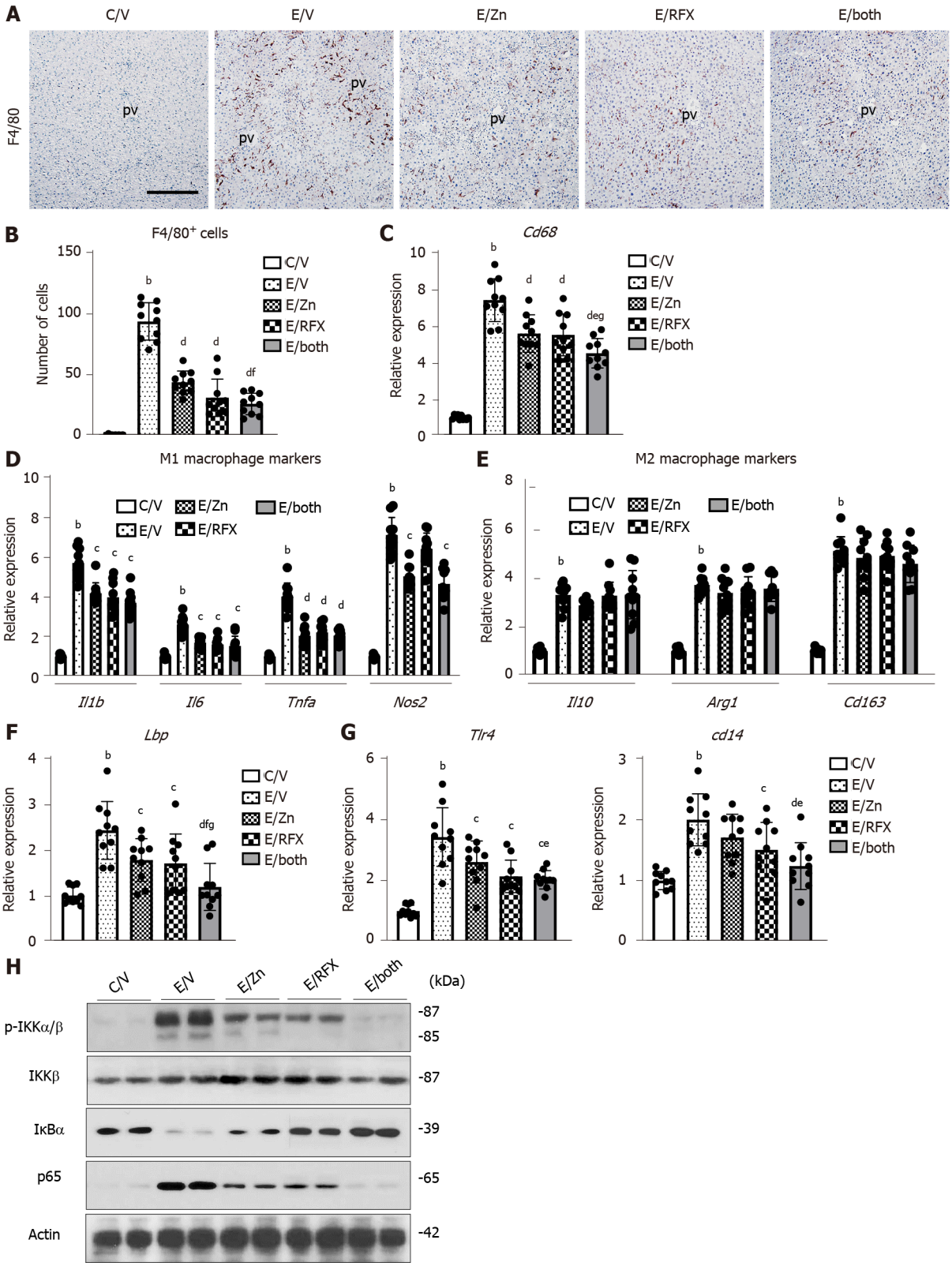


**Figure 3 Zinc acetate and rifaximin against toll-like receptor 4-mediated pro-inflammatory response in alcoholic liver disease mice.** A: Representative microphotographs of liver sections stained with F4/80. Scale bar: 50 μm. B: Semi-quantitation of F4/80 immuno-positive Kupffer cells in high-power field by NIH imageJ software. Histochemical quantitative analyses included five fields per section; C-G: Relative mRNA expression level of *Cd68* (C), M1-polarized macrophage-related genes (*Il1b*, *Il6*, *Tnfa* and *Nos2*) (D), M2-polarized macrophage-related genes (*Il10*, *Arg1* and *Cd163*) (E), *Lbp* (F), *Tlr4* and *Cd14* (G) in the liver of experimental mice. The mRNA expression levels were measured by RT-qPCR, and *Gapdh* was used as internal control. Quantitative values are indicated as fold changes to the values of C/V group; H: Western blots for p-IKKα/β, IKKβ, IkBα and NF-kB p65 in the liver of experimental mice. Actin was used as internal control. Data are mean ± SD (B-G; $n = 10$), $^{a}P < 0.05$ and $^{b}P < 0.01$ *vs* C/V group; $^{c}P < 0.05$ and $^{d}P < 0.01$ *vs* E/V group; $^{e}P < 0.05$ and $^{f}P < 0.01$ *vs* E/Zn group; $^{g}P < 0.05$ and $^{h}P < 0.01$ *vs* E/RFX group. pv: Portal vein.

inhibited these LPS-triggered accumulation of NF-kB in the ethanol plus $CCl_4$-treaed mice (Figure 3H).

### *Zinc acetate and rifaximin inhibited liver fibrosis development in ethanol plus $CCl_4$-treated mice.*

Given the antiinflammatory properties of rifaximin and zinc acetate, we evaluated their effects on the development of liver fibrosis. The ethanol plus $CCl_4$-treated mice showed extensive development of fibrous septa on Sirius Red staining (Figure 4A). Treatment with either zinc acetate or rifaximin alone significantly attenuated the ethanol plus $CCl_4$-induced fibrosis, and the antifibrotic effect was augmented by parallel use of both agents combined (Figure 4A). Correspondingly, there was a remarkable reduction in the α-SMA-immunopositive areas, which represented activation of HSCs, after treatment with zinc acetate and rifaximin (Figure 4A). Semiquantitative analysis demonstrated that the combination treatment caused more than 50% reduction in the areas of fibrotic septa and α-SMA-positive activated HSCs in the ethanol plus $CCl_4$-treated mice (Figure 4B and 4C). We also found that COL-1-immunopositive ECM deposition was decreased in parallel with the attenuation of liver fibrosis after treatment with both agents in the ethanol plus $CCl_4$-treated mice (Figure 4A and D). The western blot results substantiated that the hepatic expression of COL-1 protein was reduced *via* treatment with both agents (Figure 4E). Consistently, the hepatic gene expressions of profibrotic markers (*i.e.*, *Acta2*, *Col1a1*, and *Tgfb1*) were decreased after treatment with zinc acetate and rifaximin (Figure 4F). We further assessed the hepatic expressions of MMPs and TIMPs in the experimental groups. The ethanol plus $CCl_4$-treated mice showed increase in the hepatic mRNA levels of *Mmp2*, *Mmp9*, and *Mmp13* as liver fibrosis developed (Figure 4G). In line with the improvement of liver fibrosis, these MMP expressions were reduced after treatment with zinc acetate and rifaximin (Figure 4G). In response to this, the hepatic mRNA level of *Timp1* also varied according to liver fibrosis development (Figure 4H).

Based on the fact that zinc is essential as a component of the catalytic domain in MMPs[38], we investigated the effect of zinc supplementation on MMP activity. Interestingly, MMP-9 activity, which was indicated by active/pro MMP-9, was increased in the liver of the zinc acetate-treated groups, compared with that in the liver of the vehicle-treated group (Figure 4I).

### *Zinc acetate and rifaximin recovered the intestinal barrier function in ethanol plus $CCl_4$-treated mice*

Both zinc acetate and rifaximin efficiently prevented the accumulation of LPS in the liver, as indicated by the reduced hepatic mRNA level of *Lbp* (Figure 3D). To uncover the mechanism of these effects, we next evaluated intestinal barrier integrity in the experimental groups. In the ethanol plus $CCl_4$-treated mice, the intestinal mucosal architecture was not significantly different from that of the controls, and epithelial shedding was absent. However, there was a decrease in the villus height of the ileum mucosa in the ethanol plus $CCl_4$-treated mice (Figure 5A and B). Conversely, we found an increase in the crypt depth of the ileum in the ethanol plus $CCl_4$-treated mice (Figure 5A and C). Notably, these atrophic changes were suppressed by treatment with zinc acetate and rifaximin (Figure 5A and B). Immunofluorescent analysis showed that in the ethanol plus $CCl_4$-treated mice, the intestinal expressions of ZO-1 and Occludin, which are the markers of TJP, were markedly decreased but were effectively restored by treatment with zinc acetate and rifaximin (Figure 5A and C). The western blot results confirmed the restoration of intestinal ZO-1 and Occludin protein expressions through treatment with both agents (Figure 5D). Along with these findings, RT-qPCR analysis revealed that combination treatment with both agents increased the intestinal mRNA expressions of the other TJP markers *Cldn1*, and *Cldn4*, which encode for Claudin1, and Claudin4, respectively, as well as *Zo1* and *Ocln* (Figure 5E). To examine the functional consequence of altered cellular junctions, we determined the flux through the leak pathway, which is responsible for the paracellular movement of larger molecules, including LPS. Inversely proportional to the loss of TJPs, leakage of plasma FITC-dextran (4 kDa) increased by more than two-fold in the ethanol plus $CCl_4$-treated mice, compared with that in the control mice (Figure 5F). In correspondence with the improvement of TJP expression, leakage of FITC-dextran was significantly alleviated by treatment with both agents (Figure 5F). Moreover, we measured the intestinal mRNA levels of *Tnfα* as a downstream cytokine of TLR4, which plays a key role in ethanol-mediated disruption of the intestinal barrier function in ALD[39]. As shown in Figure 5G, intestinal *Tnfα* mRNA levels increased by three-fold in the ethanol plus $CCl_4$-treated mice, compared with those in the control

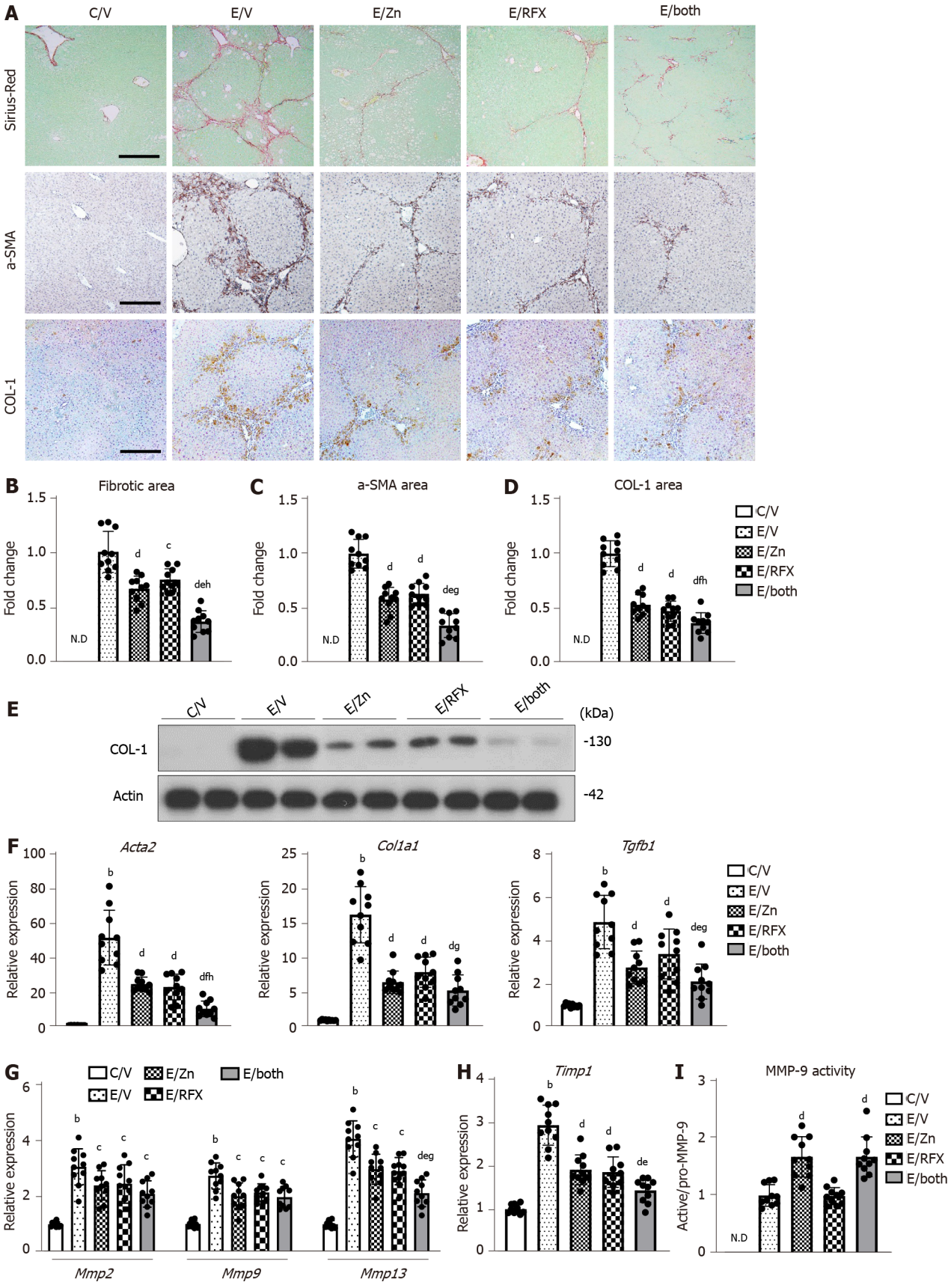


**Figure 4 Zinc acetate and rifaximin against liver fibrosis development in alcoholic liver disease mice.** A: Representative microphotographs of liver sections stained with Sirius-Red, α-smooth muscle actin (αSMA) and COL-1. Scale bar: 50 μm; B-D: Semi-quantitation of Sirius-Red-stained fibrotic area (B), α-SMA (C) and COL-1 (D) immuno-positive areas in high-power field (HPF) by NIH imageJ software. Histochemical quantitative analyses included five fields per section; E: Western blots for COL-1 in the liver of experimental mice. Actin was used as internal control; F-H: Relative mRNA expression levels of *Acta2*, *Col1a1* and *Tgfb1* (F), *Mmp-2*, *-9* and *-13* (G), and *Timp1* (H) in the liver of experimental mice. The mRNA expression levels were measured by RT-qPCR, and *Gapdh* was used

as internal control; I: Intrahepatic MMP-9 activity determined by ELISA. Quantitative values are indicated as fold changes to the values of E/V (B-D and I) or C/V group (F-H). Data are mean ± SD ($n$ = 10), [a]$P$ < 0.05 and [b]$P$ < 0.01 *vs* C/V group; [c]$P$ < 0.05 and [d]$P$ < 0.01 *vs* E/V group; [e]$P$ < 0.05 and [f]$P$ < 0.01 *vs* E/Zn group; [g]$P$ < 0.05 and [h]$P$ < 0.01 *vs* E/RFX group. ND: Not detected; αSMA: α-smooth muscle actin.

mice; moreover, combination of zinc acetate and rifaximin reduced these mRNA levels by approximately 50% of the levels after vehicle treatment (Figure 5G).

Myosin light chain kinase (MLCK) is known to play a key role in intestinal barrier disruption as a downstream target of TNFα following alcohol stimulation[40]. Therefore, we further investigated the intestinal *Mylk* mRNA levels in the experimental groups. The ethanol plus $CCl_4$-treated mice showed marked increase in the intestinal *Mylk* mRNA levels; interestingly, both zinc acetate and rifaximin reduced these mRNA levels in parallel with downregulation of TNFα (Figure 5H).

### *Direct effects of zinc acetate and rifaximin on ethanol-induced barrier dysfunction in human enterocytes*

Next, we assessed the effects of zinc acetate and rifaximin on enterocytes by *in vitro* assays using Caco-2 cells. The stimulation of 5% ethanol reduced the TEER values in the Caco-2 cells, but it did not affect cell viability (Figure 6A, B and Supplementary Figure 2A); this result indicated that this 5% ethanol-induced barrier dysfunction without cell death. The ethanol-induced reduction of TEER values was efficiently attenuated by treatment with zinc acetate, and the PI3K inhibitor LY294002 was shown to negate the zinc-mediated recovery of electrical resistance in the ethanol-stimulated Caco-2 cells (Figure 6A). It was noteworthy that rifaximin likewise dose-dependently improved the ethanol-stimulated decrease in the TEER values of the Caco-2 cells, which was sufficiently offset by treatment with a known as a PXR inhibitor SPA70 (Figure 6B). Moreover, zinc acetate or rifaximin also attenuated the LPS-stimulated decrease in the TEER values, and these attenuations were negated by treatments with LY294002 or SPA70, respectively (Figure 6C and D). At the concentrations used in the present assays, both zinc acetate and rifaximin did not affect Caco-2 cell viability (Supplementary Figure 2B). In parallel with the increase in TEER values, both zinc acetate and rifaximin restored the intestinal protein expressions of TJPs, including ZO-1 and Occludin in either ethanol- or LPS-stimulated Caco-2 cells (Figure 6E and F). Interestingly, the abovementioned methods of restoring TJPs *via* zinc acetate administration was accompanied by the augmentation of AKT phosphorylation and negated by treatments with LY294002 in either ethanol- or LPS-stimulated Caco-2 cells (Figure 6E). Notably, we found that rifaximin-mediated TJPs restoration involved the amelioration of p65 phosphorylation and negated by treatments with SPA70 in either ethanol- or LPS-stimulated Caco-2 cells (Figure 6F). These findings suggest that zinc acetate and rifaximin reintegrate the gut barrier function *via* the activation of PI3K/AKT signaling and the PXR-mediated inhibition of TLR4/NF-kB, respectively.

Additionally, the TNFα-stimulated *MYLK* expressions were not altered by treatment with zinc acetate but reduced by that with rifaximin (Figure 6G and H). Since this effect of rifaximin was also canceled by SPA-mediated PXR inhibition, rifaximin could be suggested to protect the intestinal barrier function against ethanol and LPS through PXR activation (Figure 6H).

## DISCUSSION

The gut–liver axis is an operative unit that works to protect the human body against potentially harmful substances and microorganisms, thereby, maintaining the homeostasis of the immune system[41,42]. In patients with cirrhosis, the intestine often becomes a leaky gut, which is characterized by increased permeability with defects in the intestinal TJPs[43]. Leaky gut allows the translocation of bacteria, bacterial products, and fragments, including LPS, into the portal circulation and can trigger hepatic inflammation and fibrosis[6,7,41,42]. In the present study, we elucidated that combination of zinc acetate with rifaximin additively attenuated steatosis, inflammation, and fibrosis and reduced oxidative stress in the liver of ethanol plus $CCl_4$-treated mice. As an underlying mechanism of these hepatoprotective effects mediated by both agents, we focused on the maintenance of intestinal barrier integrity, which resulted in reduced hepatic exposure of LPS.

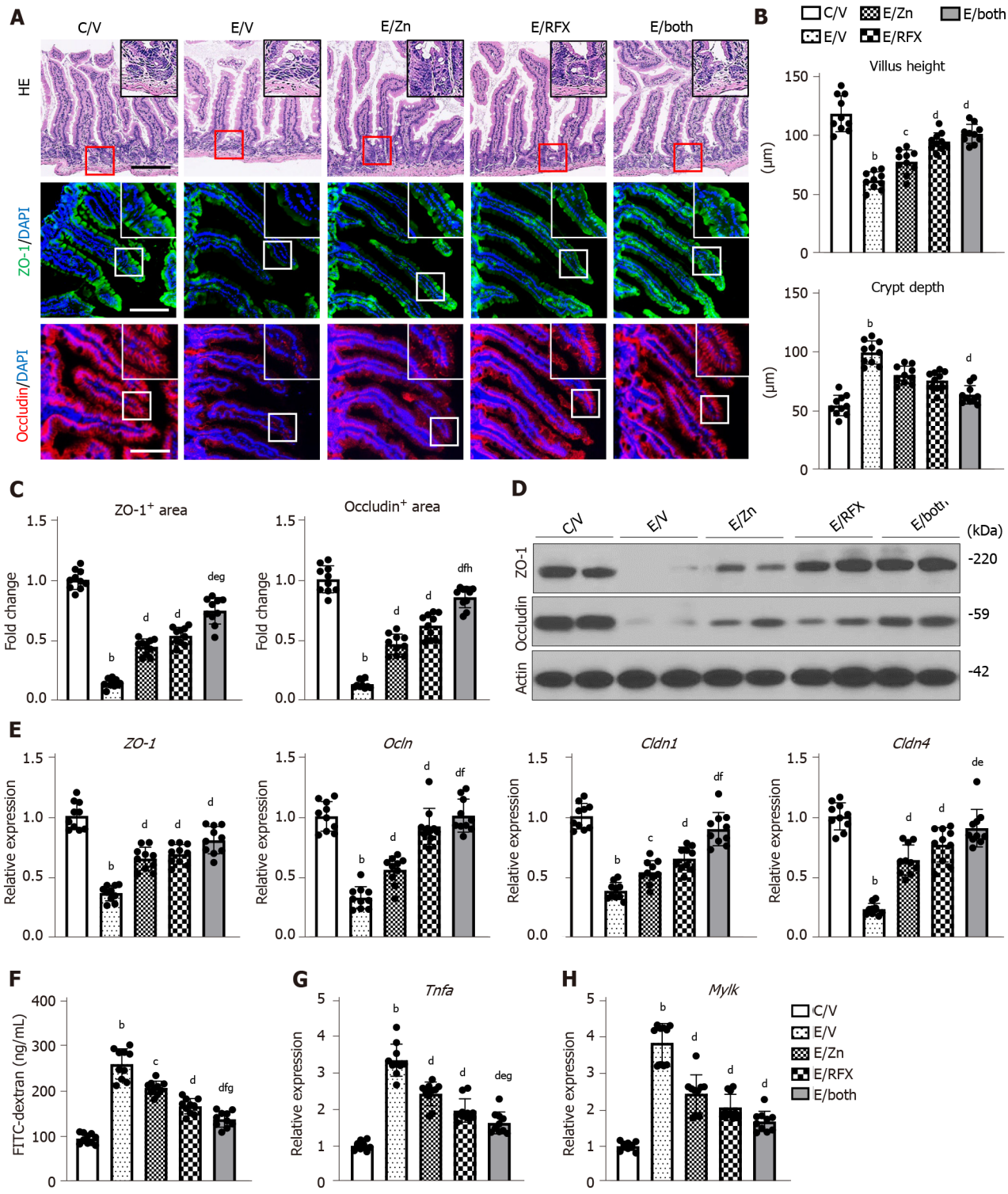


**Figure 5 Zinc acetate and rifaximin on intestinal barrier function in alcoholic liver disease mice.** A: Representative microphotographs of ileum sections stained with hematoxylin-eosin (upper), zonula occludens-1 (ZO-1) (middle) and Occludin (lower) in the experimental groups. Boxes are selected regions for magnified. Nuclei counterstained with 4',6-diamidino-2-phenylindole. Scale Bar: 50 μm; B: Villus height (upper) and crypt depth (lower) of the ileum in the experimental mice; C: Semi-quantitation of ZO-1 and Occludin immuno-positive areas in high-power field by NIH imageJ software; D: Western blots for ZO-1 and Occludin in the liver of experimental mice. Actin was used as internal control; E: Relative mRNA expression levels of *Zo1*, *Ocln*, *Cldn1* and *Cldn4* in the ileum of experimental mice; F: Blood levels of fluorescein isothiocyanate (FITC)-dextran (4kDa) 4 h after oral administration; G and H): Relative mRNA expression levels of *Tnfa* (G) and *Mylk* (H) in the ileum of experimental mice. Histochemical quantitative analyses included five fields per section (B and C). The mRNA expression levels were measured by RT-qPCR, and *Gapdh* was used as internal control (E, G and H). Quantitative values are indicated as fold changes to the values of C/V group (C, E, G and H). Data are mean ± SD (B, C, E, G and H; $n = 10$, F; $n = 5$), $^{a}P < 0.05$ and $^{b}P < 0.01$ *vs* C/V group; $^{c}P < 0.05$ and $^{d}P < 0.01$ *vs* E/V group; $^{e}P < 0.05$ and $^{f}P < 0.01$ *vs* E/Zn group; $^{g}P < 0.05$ and $^{h}P < 0.01$ *vs* E/RFX group. DAPI: 4',6-diamidino-2-phenylindole; ZO-1: Zonula occludens; HE: Hematoxylin and eosin.

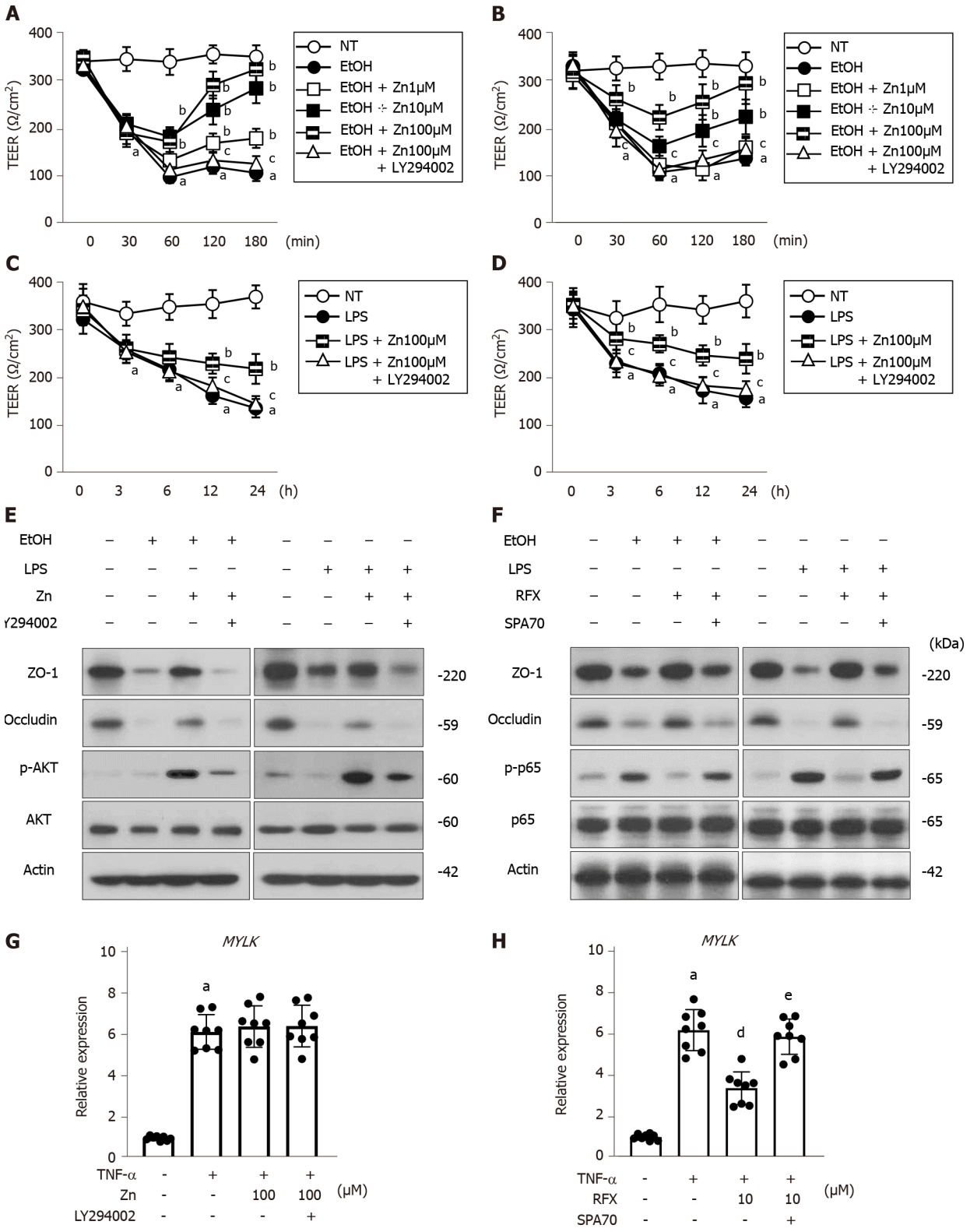


**Figure 6 Effects of zinc acetate and rifaximin on *in vitro* EtOH/LPS/TNF-α-stimulated Caco-2 cells.** A-D: *In vitro* paracellular permeability in ethanol (EtOH) (A and B)- or lipopolysaccharide (LPS) (C and D)-stimulated Caco-2 cells determined as transepithelial electrical resistance; E and F: Western blots for the effects of zinc acetate (100 μM) on ZO-1, Occludin, p-AKT and AKT expressions (E) and rifaximin (10 μM) on ZO-1, Occludin, p-p65 and p65 expressions (F) in the whole cell lysate of Caco-2 cells. Actin was used as internal control; G and H: Relative mRNA expression levels of *MYLK* in TNF-α-stimulated Caco-2 cells. The mRNA expression levels were measured by RT-qPCR, and *GAPDH* was used as internal control. Quantitative values are indicated as fold changes to the values of non-treatment group. Caco-2 were treated with each agent as following; (A, C, E and G) zinc acetate (Zn) and/or PI3K inhibitor, LY294002, (B, D, F and H) rifaximin (RFX) and/or human PXR inhibitor, SPA70. Data are mean ± SD (A-D; $n = 6$, G and H; $n = 8$), $^{a}P < 0.01$ *vs* non-treated groups (A-D, G and H), $^{b}P < 0.01$ *vs* EtOH (A and B) or LPS-treated groups (C and D), $^{c}P < 0.01$ *vs* EtOH with Zn (100 μM) (A), EtOH with RFX (10 μM) (B), LPS with Zn (100 μM) (C) or LPS with RFX (10 μM) (D)-treated groups, $^{d}P < 0.01$ *vs* TNF-α-treated group (H), $^{e}P < 0.01$ *vs* TNF-α with RFX (10 μM)-treated group (H). LPS: Lipopolysaccharide; TEER: Transepithelial electrical resistance; EtOH: Ethanol; ZO-1: Zonula occludens.

The presence of alcohol and its metabolites, such as acetaldehyde, in the bloodstream is known to injure intestinal epithelial cells directly and indirectly[44]. Alcohol binge at high concentrations causes intestinal cellular damage, and chronic exposure to ethanol decreases the expressions of TJPs in between colon epithelial cells [44]. In this context, recent clinical evidences have shown that acute alcohol binge drinking significantly increased serum endotoxin levels in healthy human volunteers and that serum endotoxin was elevated in patients with chronic alcohol consumption and ALD[45,46]. A previous study on rodents showed that exposure of ethanol and $CCl_4$ reduced the diversity of gut microbiota which resulted in bacterial translocation [47]. Similarly, our current model was observed to have remarkable increase in the hepatic *Lbp* expression, in accordance with decreased intestinal TJP expression and increased leakage of plasma FITC-dextran, which indicated augmentation of LPS exposure to the liver along with intestinal hyperpermeability. These features were supported by our results on the *in vitro* assay, which showed that the ethanol-stimulus profoundly weakened epithelial resistance and reduced TJP expressions in Caco-2 cells, in agreement with previous reports.

Our therapeutic models showed that both zinc acetate and rifaximin reinforced the tight junctions in the intestine of ethanol plus $CCl_4$-treated mice. We assumed the involvement of multifunctional pathways in these effects of both agents (Figure 7). First, both drugs suppressed the intestinal TNFα and MLCK expressions in mice. Chen *et al*[40] demonstrated that dysbiosis triggered by chronic alcohol administration induced TNFα production in the inflammatory cells of the intestinal lamina propria and that the TNFα/TNF receptor I axis potentially regulated tight junction disruption through activation of MLCK. Thus, the decrease of intestinal TNFα mediated by both agents participates in the improved intestinal barrier function. Moreover, Garg *et al*[48] documented that rifaximin attenuated TNFα-induced MLCK expression through PXR activation in human enterocytes. Accordingly, our *in vitro* assay in Caco-2 cells validated the inhibitory effect of rifaximin on TNFα-stimulated upregulation of MLCK through PXR activation. These results indicated that suppression of TNFα/MLCK pathway was partially associated with the reinforced tight junctions in the ethanol plus $CCl_4$-treated mice. Second, both zinc acetate and rifaximin also improved the LPS-stimulated intestinal barrier dysfunction. Zinc has been reported to enhance intestinal epithelial barrier function by directly affecting enterocytes through activation of PI3K/AKT/mTOR signaling[34]. He *et al*[49] demonstrated that the pharmacological activation of PI3K/AKT could inhibit the LPS-induced downregulation of TJP expressions in Caco-2 cells. Meanwhile, rifaximin-mediated PXR activation has been suggested to attenuate the LPS-stimulated barrier dysfunction in intestinal epithelial cells through the inhibition of TLR4/NF-kB p65 pathway as well as the abovementioned TNFα/MLCK pathway[50]. Consistently, our *in vitro* study found that zinc acetate or rifaximin suppressed the LPS-stimulated disruption of intestinal barrier function, which was mitigated by inhibition of PI3K or PXR, respectively in the Caco-2 cells. These findings support that both agents protect the intestinal barrier breakdown triggered by LPS. Other than the above, a variety of molecular mechanisms have been supposed to be relevant to the zinc-mediated alteration of intestinal barrier permeability and TJP expression. Zinc-induced activation of different signaling pathways such as PKCd or MAPK/ERK has been reported to improve epithelial integrity[51,52]. Moreover, dietary zinc supplementation could promote the metabolism of acetaldehyde in the gut by enhancing ALDH1B1 activity[53]. To explore the possible involvement of these molecular mechanisms in the present model, further investigations are required.

In addition to intestinal barrier maintenance, several pharmacologic actions have been suggested to be associated with the antifibrotic properties of zinc. Szuster-Ciesielska *et al*[54] demonstrated that zinc supplementation could silence ethanol- or acetaldehyde-mediated HSC activation by acting as an antioxidant and inhibitor of MAPK, TGFβ, and NF-kB transduction signaling. In our models, the increased hepatic zinc levels and hepatic MMP-9 activity after zinc acetate treatment implied that the antifibrotic effect was at least partially associated with a direct effect on the profibrogenic activity of HSCs. However, detailed consideration by analyzing the molecular mechanisms in HSCs isolated from the liver of the experimental groups would be needed.

When considering the results of this study, several important limitations should be acknowledged. First, although our study addressed the effects of zinc acetate and rifaximin on intestinal barrier integrity in the ethanol plus $CCl_4$-treated mice, their effects on microbial profiles were not clarified. Several studies have indicated the impacts of both agents on the gut microbiota. Zhang *et al*[55] showed that zinc modified the cecal microbial community in broilers by making abundant in the

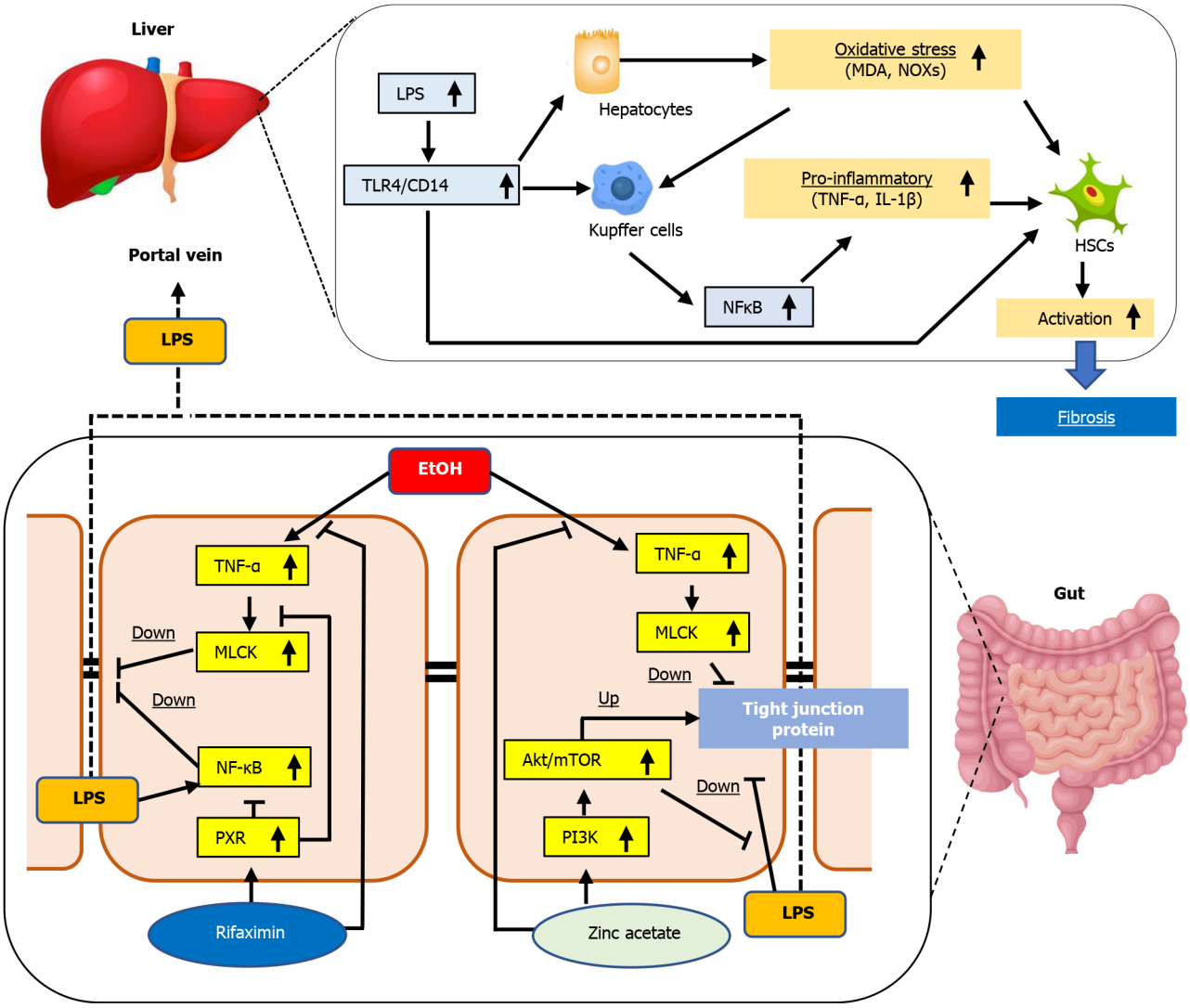


**Figure 7 Graphic summary of the effect of zinc acetate and rifaximin on the alcoholic liver disease-related liver fibrosis.** ALD: Alcoholic liver disease; TLR4: Toll-like receptor 4; MDA: Malondialdehyde; LPS: Lipopolysaccharide; HSC: Hepatic stellate cell; TNFα: Tumor necrosis factor α; MLCK: Myosin light chain kinase; NF-kB: Nuclear factor kB; PXR: Pregnane X receptor.

populations of total bacteria, including Lactobacillus, and reducing the populations of Salmonella. Foligné *et al*[56] suggested that zinc supplementation provided a significant increase in endogenous Clostridiaceae in mice. Meanwhile, in a mouse steatohepatitis model, Kitagawa *et al*[27] have recently demonstrated that rifaximin improved ethanol-induced liver injury with drastic modification of the small intestine microbiota; they elucidated that rifaximin decreased the relative abundance of Erysipelotrichales and increased Bacteroidales. Given these evidences, additional analyses are necessary to determine the interaction between microbial alterations by both agents and the therapeutic effects in our model. Second, this study elucidated the preventive effects of zinc acetate and rifaximin on the progression of ethanol plus $CCl_4$ -induced liver fibrosis; however, the pharmacologic properties of fibrinolysis and liver regeneration in an established model of liver fibrosis remain obscure. Future studies should address whether both drugs could induce fibrinolysis and efficient liver regeneration in other models of cirrhosis.

## CONCLUSION

Taken together, our results indicated that combination of zinc acetate and rifaximin exerted a preventive effect on the ALD-related liver fibrosis in a mouse model treated with ethanol plus $CCl_4$. We believed that this antifibrotic effect is involved in the multifaceted regulatory functions that maintain intestinal barrier integrity and reduce

hepatic LPS exposure, thereby, leading to Kupffer cell expansion and HSC activation by inhibition of the TLR4 signaling pathway. We emphasize that both drugs are clinically available for patients with chronic liver diseases and that the abovementioned effects on alcohol-related liver fibrosis were achieved using the pharmacologic doses, without adverse effects, such as hypocupremia or renal dysfunction. Therefore, the results of this study demonstrated that this combination regimen could be beneficial as a form of chemoprevention against alcohol-related liver fibrosis.

## ARTICLE HIGHLIGHTS

### *Research background*

Liver fibrosis related to alcoholic liver disease (ALD) is one of the most critical health issues. Alcohol cessation is the therapeutic mainstay for patients with all stages of ALD, whereas pharmacological strategies for liver fibrosis have not been established. It has been recognized that the gut-derived endotoxin lipopolysaccharide (LPS), which is a key player of gut-liver axis, particularly exacerbates the inflammation and fibrosis *via* activation of toll-like receptor 4 (TLR4)/nuclear factor kB (NF-kB) signaling pathway in ALD. Thus, blockage of the transfer of LPS to the liver by maintaining gut barrier has gained attention for a therapeutic strategy to prevent ALD-related liver fibrosis.

### *Research motivation*

Currently, zinc acetate and rifaximin are often used for the cirrhotic patients in the clinical practice. Several clinical and basic studies have demonstrated that both agents also could suppress the intestinal hyperpermeability. Although these evidences suggest that combination of zinc acetate and rifaximin should exert beneficial effects on the ALD-related liver fibrosis through inhibition of LPS/TLR4/NF-kB signaling, its effects on ALD-related liver fibrosis remain to be fully elucidated.

### *Research objectives*

To determine the efficacy of dual therapy with zinc acetate and rifaximin for liver fibrosis and explore its underlying mechanisms with the linkage of gut barrier function in a mouse ALD model.

### *Research methods*

Female C57BL/6J mice were fed a 2.5% ethanol-containing liquid diet and administered carbon tetrachloride (CCl4) twice weekly (1 mL/kg; ip) for 8 wk to induce ALD-related liver fibrosis, and zinc acetate (100 mg/L) and/or rifaximin (100 mg/L) were orally administered during experimental period. Histological changes in hepatic steatosis, inflammation and fibrosis, oxidative markers, and LPS/TLR4/NF-kB signaling as well as intestinal permeability and tight junction proteins (TJPs) were evaluated. Additionally, *in vitro* assays were performed to investigate the direct effects of both agents on Caco-2 barrier function.

### *Research results*

The ethanol plus $CCl_4$-treated mice showed significantly increased transaminases, hepatic fat accumulation, lipid peroxidation (malondialdehyde), F4/80-positive Kupffer cell expansion and increased proinflammatory response, liver fibrosis development and HSC activation. The combination with zinc acetate and rifaximin attenuated these phenotypic changes with with blunted hepatic exposure of LPS and the TLR4/NF-kB signaling pathway. This combination therapy improved the atrophic changes and permeability in the ileum and restored the TJPs (ZO-1, Occludin, Claudin1 and Claudin4) with decreased levels of tumor necrosis factor α and myosin light chain kinase. Moreover, *in vitro* assay revealed that zinc acetate and rifaximin directly reinforced ethanol or LPS-stimulated paracellular permeability and upregulated TJPs in Caco-2 cells by modulating different pathways, *i.e.*, induction of AKT phosphorylation by zinc acetate and pregnane X receptor activation by rifaximin.

### *Research conclusions*

The combination of zinc acetate and rifaximin exerted a preventive effect on the ALD-related liver fibrosis in a mouse ALD model by maintaining intestinal barrier integrity and reduce hepatic LPS exposure, thereby, leading to Kupffer cell expansion and HSC activation by inhibition of the TLR4 signaling pathway.

### *Research perspectives*

By indicating that zinc acetate and rifaximin inhibits ALD-related liver fibrosis development through the gut-liver axis, the results of this study demonstrated that this combination regimen could be beneficial as a form of chemoprevention against ALD-related liver fibrosis.

## REFERENCES


1 **Younossi Z**, Henry L. Contribution of Alcoholic and Nonalcoholic Fatty Liver Disease to the Burden of Liver-Related Morbidity and Mortality. *Gastroenterology* 2016; **150**: 1778-1785 [PMID: 26980624 DOI: 10.1053/j.gastro.2016.03.005]

2 **Williams R**, Alexander G, Armstrong I, Baker A, Bhala N, Camps-Walsh G, Cramp ME, de Lusignan S, Day N, Dhawan A, Dillon J, Drummond C, Dyson J, Foster G, Gilmore I, Hudson M, Kelly D, Langford A, McDougall N, Meier P, Moriarty K, Newsome P, O'Grady J, Pryke R, Rolfe L, Rice P, Rutter H, Sheron N, Taylor A, Thompson J, Thorburn D, Verne J, Wass J, Yeoman A. Disease burden and costs from excess alcohol consumption, obesity, and viral hepatitis: fourth report of the Lancet Standing Commission on Liver Disease in the UK. *Lancet* 2018; **391**: 1097-1107 [PMID: 29198562 DOI: 10.1016/S0140-6736(17)32866-0]

3 **Liangpunsakul S**, Haber P, McCaughan GW. Alcoholic Liver Disease in Asia, Europe, and North America. *Gastroenterology* 2016; **150**: 1786-1797 [PMID: 26924091 DOI: 10.1053/j.gastro.2016.02.043]

4 **Seitz HK**, Bataller R, Cortez-Pinto H, Gao B, Gual A, Lackner C, Mathurin P, Mueller S, Szabo G, Tsukamoto H. Alcoholic liver disease. *Nat Rev Dis Primers* 2018; **4**: 16 [PMID: 30115921 DOI: 10.1038/s41572-018-0014-7]

5 **Louvet A**, Mathurin P. Alcoholic liver disease: mechanisms of injury and targeted treatment. *Nat Rev Gastroenterol Hepatol* 2015; **12**: 231-242 [PMID: 25782093 DOI: 10.1038/nrgastro.2015.35]

6 **Bajaj JS**. Alcohol, liver disease and the gut microbiota. *Nat Rev Gastroenterol Hepatol* 2019; **16**: 235-246 [PMID: 30643227 DOI: 10.1038/s41575-018-0099-1]

7 **Szabo G**. Gut-liver axis in alcoholic liver disease. *Gastroenterology* 2015; **148**: 30-36 [PMID: 25447847 DOI: 10.1053/j.gastro.2014.10.042]

8 **Ciesielska A**, Matyjek M, Kwiatkowska K. TLR4 and CD14 trafficking and its influence on LPS-induced pro-inflammatory signaling. *Cell Mol Life Sci* 2021; **78**: 1233-1261 [PMID: 33057840 DOI: 10.1007/s00018-020-03656-y]

9 **Seki E**, De Minicis S, Osterreicher CH, Kluwe J, Osawa Y, Brenner DA, Schwabe RF. TLR4 enhances TGF-beta signaling and hepatic fibrosis. *Nat Med* 2007; **13**: 1324-1332 [PMID: 17952090 DOI: 10.1038/nm1663]

10 **Maret W**. Zinc biochemistry: from a single zinc enzyme to a key element of life. *Adv Nutr* 2013; **4**: 82-91 [PMID: 23319127 DOI: 10.3945/an.112.003038]

11 **Zhou Z**. Zinc and alcoholic liver disease. *Dig Dis* 2010; **28**: 745-750 [PMID: 21525759 DOI: 10.1159/000324282]

12 **Wu J**, Meng QH. Current understanding of the metabolism of micronutrients in chronic alcoholic liver disease. *World J Gastroenterol* 2020; **26**: 4567-4578 [PMID: 32884217 DOI: 10.3748/wjg.v26.i31.4567]

13 **Shen YC**, Chang YH, Fang CJ, Lin YS. Zinc supplementation in patients with cirrhosis and hepatic encephalopathy: a systematic review and meta-analysis. *Nutr J* 2019; **18**: 34 [PMID: 31279342 DOI: 10.1186/s12937-019-0461-3]

14 **Himoto T**, Masaki T. Associations between Zinc Deficiency and Metabolic Abnormalities in Patients with Chronic Liver Disease. *Nutrients* 2018; **10** [PMID: 29342898 DOI: 10.3390/nu10010088]

15 **Moriya K**, Nishimura N, Namisaki T, Takaya H, Sawada Y, Kawaratani H, Kaji K, Shimozato N, Sato S, Furukawa M, Douhara A, Akahane T, Mitoro A, Yamao J, Yoshiji H. Zinc Administration and Improved Serum Markers of Hepatic Fibrosis in Patients with Autoimmune Hepatitis. *J Clin Med* 2021; **10** [PMID: 34199421 DOI: 10.3390/jcm10112465]

16 **Zhong W**, Wei X, Hao L, Lin TD, Yue R, Sun X, Guo W, Dong H, Li T, Ahmadi AR, Sun Z, Zhang Q, Zhao J, Zhou Z. Paneth Cell Dysfunction Mediates Alcohol-related Steatohepatitis Through Promoting Bacterial Translocation in Mice: Role of Zinc Deficiency. *Hepatology* 2020; **71**: 1575-1591 [PMID: 31520476 DOI: 10.1002/hep.30945]

17 **Sun J**, Zhang C, Zhang B. Research Note: Effects of organic zinc on broiler intestinal permeability and integrity in Clostridium perfringens-challenged condition. *Poult Sci* 2020; **99**: 6653-6656 [PMID: 33248581 DOI: 10.1016/j.psj.2020.09.032]

18 **Lambert JC**, Zhou Z, Wang L, Song Z, McClain CJ, Kang YJ. Prevention of alterations in intestinal permeability is involved in zinc inhibition of acute ethanol-induced liver damage in mice. *J Pharmacol Exp Ther* 2003; **305**: 880-886 [PMID: 12626662 DOI: 10.1124/jpet.102.047852]

19 **Tan HK**, Streeter A, Cramp ME, Dhanda AD. Effect of zinc treatment on clinical outcomes in patients with liver cirrhosis: A systematic review and meta-analysis. *World J Hepatol* 2020; **12**: 389-398 [PMID: 32821337 DOI: 10.4254/wjh.v12.i7.389]

20 **DuPont HL**. Travelers' diarrhea: antimicrobial therapy and chemoprevention. *Nat Clin Pract Gastroenterol Hepatol* 2005; **2**: 191-8; quiz 1 p following 198 [PMID: 16265184 DOI:

10.1038/ncpgasthep0142]
21 **Moran S**, López-Sánchez M, Milke-García MDP, Rodríguez-Leal G. Current approach to treatment of minimal hepatic encephalopathy in patients with liver cirrhosis. *World J Gastroenterol* 2021; **27**: 3050-3063 [PMID: 34168407 DOI: 10.3748/wjg.v27.i22.3050]
22 **Kaji K**, Takaya H, Saikawa S, Furukawa M, Sato S, Kawaratani H, Kitade M, Moriya K, Namisaki T, Akahane T, Mitoro A, Yoshiji H. Rifaximin ameliorates hepatic encephalopathy and endotoxemia without affecting the gut microbiome diversity. *World J Gastroenterol* 2017; **23**: 8355-8366 [PMID: 29307995 DOI: 10.3748/wjg.v23.i47.8355]
23 **Esposito G**, Nobile N, Gigli S, Seguella L, Pesce M, d'Alessandro A, Bruzzese E, Capoccia E, Steardo L, Cuomo R, Sarnelli G. Rifaximin Improves Clostridium difficile Toxin A-Induced Toxicity in Caco-2 Cells by the PXR-Dependent TLR4/MyD88/NF-kB Pathway. *Front Pharmacol* 2016; **7**: 120 [PMID: 27242527 DOI: 10.3389/fphar.2016.00120]
24 **Ishida K**, Kaji K, Sato S, Ogawa H, Takagi H, Takaya H, Kawaratani H, Moriya K, Namisaki T, Akahane T, Yoshiji H. Sulforaphane ameliorates ethanol plus carbon tetrachloride-induced liver fibrosis in mice through the Nrf2-mediated antioxidant response and acetaldehyde metabolization with inhibition of the LPS/TLR4 signaling pathway. *J Nutr Biochem* 2021; **89**: 108573 [PMID: 33388347 DOI: 10.1016/j.jnutbio.2020.108573]
25 **Roychowdhury S**, Chiang DJ, McMullen MR, Nagy LE. Moderate, chronic ethanol feeding exacerbates carbon-tetrachloride-induced hepatic fibrosis *via* hepatocyte-specific hypoxia inducible factor 1α. *Pharmacol Res Perspect* 2014; **2**: e00061 [PMID: 25089199 DOI: 10.1002/prp2.61]
26 **Johnson JK**, Harris FL, Ping XD, Gauthier TW, Brown LAS. Role of zinc insufficiency in fetal alveolar macrophage dysfunction and RSV exacerbation associated with fetal ethanol exposure. *Alcohol* 2019; **80**: 5-16 [PMID: 30580016 DOI: 10.1016/j.alcohol.2018.11.007]
27 **Kitagawa R**, Kon K, Uchiyama A, Arai K, Yamashina S, Kuwahara-Arai K, Kirikae T, Ueno T, Ikejima K. Rifaximin prevents ethanol-induced liver injury in obese KK-A$^{y}$ mice through modulation of small intestinal microbiota signature. *Am J Physiol Gastrointest Liver Physiol* 2019; **317**: G707-G715 [PMID: 31509430 DOI: 10.1152/ajpgi.00372.2018]
28 **Her Z**, Tan JHL, Lim YS, Tan SY, Chan XY, Tan WWS, Liu M, Yong KSM, Lai F, Ceccarello E, Zheng Z, Fan Y, Chang KTE, Sun L, Chang SC, Chin CL, Lee GH, Dan YY, Chan YS, Lim SG, Chan JKY, Chandy KG, Chen Q. CD4$^{+}$ T Cells Mediate the Development of Liver Fibrosis in High Fat Diet-Induced NAFLD in Humanized Mice. *Front Immunol* 2020; **11**: 580968 [PMID: 33013934 DOI: 10.3389/fimmu.2020.580968]
29 **Luciano-Mateo F**, Cabré N, Fernández-Arroyo S, Baiges-Gaya G, Hernández-Aguilera A, Rodríguez-Tomàs E, Muñoz-Pinedo C, Menéndez JA, Camps J, Joven J. Chemokine C-C motif ligand 2 overexpression drives tissue-specific metabolic responses in the liver and muscle of mice. *Sci Rep* 2020; **10**: 11954 [PMID: 32686726 DOI: 10.1038/s41598-020-68769-7]
30 **Suzuki M**, Kon K, Ikejima K, Arai K, Uchiyama A, Aoyama T, Yamashina S, Ueno T, Watanabe S. The Chemical Chaperone 4-Phenylbutyric Acid Prevents Alcohol-Induced Liver Injury in Obese KK-A$^{y}$ Mice. *Alcohol Clin Exp Res* 2019; **43**: 617-627 [PMID: 30748014 DOI: 10.1111/acer.13982]
31 **Matheus VA**, Monteiro L, Oliveira RB, Maschio DA, Collares-Buzato CB. Butyrate reduces high-fat diet-induced metabolic alterations, hepatic steatosis and pancreatic beta cell and intestinal barrier dysfunctions in prediabetic mice. *Exp Biol Med (Maywood)* 2017; **242**: 1214-1226 [PMID: 28504618 DOI: 10.1177/1535370217708188]
32 **Hossain KFB**, Akter M, Rahman MM, Sikder MT, Rahaman MS, Yamasaki S, Kimura G, Tomihara T, Kurasaki M, Saito T. Amelioration of Metal-Induced Cellular Stress by α-Lipoic Acid and Dihydrolipoic Acid through Antioxidative Effects in PC12 Cells and Caco-2 Cells. *Int J Environ Res Public Health* 2021; **18** [PMID: 33671655 DOI: 10.3390/ijerph18042126]
33 **Wang Y**, Tong J, Chang B, Wang B, Zhang D. Effects of alcohol on intestinal epithelial barrier permeability and expression of tight junction-associated proteins. *Mol Med Rep* 2014; **9**: 2352-2356 [PMID: 24718485 DOI: 10.3892/mmr.2014.2126]
34 **Shao Y**, Wolf PG, Guo S, Guo Y, Gaskins HR, Zhang B. Zinc enhances intestinal epithelial barrier function through the PI3K/AKT/mTOR signaling pathway in Caco-2 cells. *J Nutr Biochem* 2017; **43**: 18-26 [PMID: 28193579 DOI: 10.1016/j.jnutbio.2017.01.013]
35 **Lin W**, Wang YM, Chai SC, Lv L, Zheng J, Wu J, Zhang Q, Wang YD, Griffin PR, Chen T. SPA70 is a potent antagonist of human pregnane X receptor. *Nat Commun* 2017; **8**: 741 [PMID: 28963450 DOI: 10.1038/s41467-017-00780-5]
36 **Nishii N**, Oshima T, Li M, Eda H, Nakamura K, Tamura A, Ogawa T, Yamasaki T, Kondo T, Kono T, Tozawa K, Tomita T, Fukui H, Miwa H. Lubiprostone Induces Claudin-1 and Protects Intestinal Barrier Function. *Pharmacology* 2020; **105**: 102-108 [PMID: 31536982 DOI: 10.1159/000503054]
37 **Tsuji Y**, Kaji K, Kitade M, Kaya D, Kitagawa K, Ozutsumi T, Fujinaga Y, Takaya H, Kawaratani H, Namisaki T, Moriya K, Akahane T, Yoshiji H. Bile Acid Sequestrant, Sevelamer Ameliorates Hepatic Fibrosis with Reduced Overload of Endogenous Lipopolysaccharide in Experimental Nonalcoholic Steatohepatitis. *Microorganisms* 2020; **8** [PMID: 32575352 DOI: 10.3390/microorganisms8060925]
38 **Kumar H**, Mandal SK, Gogoi P, Kanaujia SP. Structural and functional role of invariant water molecules in matrix metalloproteinases: a data-mining approach. *J Biomol Struct Dyn* 2021; 1-12 [PMID: 34121627 DOI: 10.1080/07391102.2021.1938683]
39 **Fleming S**, Toratani S, Shea-Donohue T, Kashiwabara Y, Vogel SN, Metcalf ES. Pro- and anti-inflammatory gene expression in the murine small intestine and liver after chronic exposure to alcohol. *Alcohol Clin Exp Res* 2001; **25**: 579-589 [PMID: 11329499]

40 **Chen P**, Stärkel P, Turner JR, Ho SB, Schnabl B. Dysbiosis-induced intestinal inflammation activates tumor necrosis factor receptor I and mediates alcoholic liver disease in mice. *Hepatology* 2015; **61**: 883-894 [PMID: 25251280 DOI: 10.1002/hep.27489]

41 **Wang R**, Tang R, Li B, Ma X, Schnabl B, Tilg H. Gut microbiome, liver immunology, and liver diseases. *Cell Mol Immunol* 2021; **18**: 4-17 [PMID: 33318628 DOI: 10.1038/s41423-020-00592-6]

42 **Trebicka J**, Macnaughtan J, Schnabl B, Shawcross DL, Bajaj JS. The microbiota in cirrhosis and its role in hepatic decompensation. *J Hepatol* 2021; **75** Suppl 1: S67-S81 [PMID: 34039493 DOI: 10.1016/j.jhep.2020.11.013]

43 **Assimakopoulos SF**, Tsamandas AC, Tsiaoussis GI, Karatza E, Triantos C, Vagianos CE, Spiliopoulou I, Kaltezioti V, Charonis A, Nikolopoulou VN, Scopa CD, Thomopoulos KC. Altered intestinal tight junctions' expression in patients with liver cirrhosis: a pathogenetic mechanism of intestinal hyperpermeability. *Eur J Clin Invest* 2012; **42**: 439-446 [PMID: 22023490 DOI: 10.1111/j.1365-2362.2011.02609.x]

44 **Bishehsari F**, Magno E, Swanson G, Desai V, Voigt RM, Forsyth CB, Keshavarzian A. Alcohol and Gut-Derived Inflammation. *Alcohol Res* 2017; **38**: 163-171 [PMID: 28988571]

45 **Bala S**, Marcos M, Gattu A, Catalano D, Szabo G. Acute binge drinking increases serum endotoxin and bacterial DNA levels in healthy individuals. *PLoS One* 2014; **9**: e96864 [PMID: 24828436 DOI: 10.1371/journal.pone.0096864]

46 **Bode C**, Bode JC. Effect of alcohol consumption on the gut. *Best Pract Res Clin Gastroenterol* 2003; **17**: 575-592 [PMID: 12828956 DOI: 10.1016/s1521-6918(03)00034-9]

47 **Furuya S**, Cichocki JA, Konganti K, Dreval K, Uehara T, Katou Y, Fukushima H, Kono H, Pogribny IP, Argemi J, Bataller R, Rusyn I. Histopathological and Molecular Signatures of a Mouse Model of Acute-on-Chronic Alcoholic Liver Injury Demonstrate Concordance With Human Alcoholic Hepatitis. *Toxicol Sci* 2019; **170**: 427-437 [PMID: 30517762 DOI: 10.1093/toxsci/kfy292]

48 **Garg A**, Zhao A, Erickson SL, Mukherjee S, Lau AJ, Alston L, Chang TK, Mani S, Hirota SA. Pregnane X Receptor Activation Attenuates Inflammation-Associated Intestinal Epithelial Barrier Dysfunction by Inhibiting Cytokine-Induced Myosin Light-Chain Kinase Expression and c-Jun N-Terminal Kinase 1/2 Activation. *J Pharmacol Exp Ther* 2016; **359**: 91-101 [PMID: 27440420 DOI: 10.1124/jpet.116.234096]

49 **He S**, Guo Y, Zhao J, Xu X, Wang N, Liu Q. Ferulic Acid Ameliorates Lipopolysaccharide-Induced Barrier Dysfunction *via* MicroRNA-200c-3p-Mediated Activation of PI3K/AKT Pathway in Caco-2 Cells. *Front Pharmacol* 2020; **11**: 376 [PMID: 32308620 DOI: 10.3389/fphar.2020.00376]

50 **Mencarelli A**, Renga B, Palladino G, Claudio D, Ricci P, Distrutti E, Barbanti M, Baldelli F, Fiorucci S. Inhibition of NF-kB by a PXR-dependent pathway mediates counter-regulatory activities of rifaximin on innate immunity in intestinal epithelial cells. *Eur J Pharmacol* 2011; **668**: 317-324 [PMID: 21806984 DOI: 10.1016/j.ejphar.2011.06.058]

51 **Shao YX**, Lei Z, Wolf PG, Gao Y, Guo YM, Zhang BK. Zinc Supplementation, *via* GPR39, Upregulates PKCζ to Protect Intestinal Barrier Integrity in Caco-2 Cells Challenged by *Salmonella enterica* Serovar Typhimurium. *J Nutr* 2017; **147**: 1282-1289 [PMID: 28515165 DOI: 10.3945/jn.116.243238]

52 **Sarkar P**, Saha T, Sheikh IA, Chakraborty S, Aoun J, Chakrabarti MK, Rajendran VM, Ameen NA, Dutta S, Hoque KM. Zinc ameliorates intestinal barrier dysfunctions in shigellosis by reinstating claudin-2 and -4 on the membranes. *Am J Physiol Gastrointest Liver Physiol* 2019; **316**: G229-G246 [PMID: 30406698 DOI: 10.1152/ajpgi.00092.2018]

53 **Zhong W**, Li Q, Sun Q, Zhang W, Zhang J, Sun X, Yin X, Zhang X, Zhou Z. Preventing Gut Leakiness and Endotoxemia Contributes to the Protective Effect of Zinc on Alcohol-Induced Steatohepatitis in Rats. *J Nutr* 2015; **145**: 2690-2698 [PMID: 26468492 DOI: 10.3945/jn.115.216093]

54 **Szuster-Ciesielska A**, Plewka K, Daniluk J, Kandefer-Szerszeń M. Zinc supplementation attenuates ethanol- and acetaldehyde-induced liver stellate cell activation by inhibiting reactive oxygen species (ROS) production and by influencing intracellular signaling. *Biochem Pharmacol* 2009; **78**: 301-314 [PMID: 19376089 DOI: 10.1016/j.bcp.2009.04.009]

55 **Zhang B**, Shao Y, Liu D, Yin P, Guo Y, Yuan J. Zinc prevents Salmonella enterica serovar Typhimurium-induced loss of intestinal mucosal barrier function in broiler chickens. *Avian Pathol* 2012; **41**: 361-367 [PMID: 22834550 DOI: 10.1080/03079457.2012.692155]

56 **Foligné B**, George F, Standaert A, Garat A, Poiret S, Peucelle V, Ferreira S, Sobry H, Muharram G, Lucau-Danila A, Daniel C. High-dose dietary supplementation with zinc prevents gut inflammation: Investigation of the role of metallothioneins and beyond by transcriptomic and metagenomic studies. *FASEB J* 2020; **34**: 12615-12633 [PMID: 32729971 DOI: 10.1096/fj.202000562RR]